



Quenching rates and critical densities of $c\text{-C}_3\text{H}_2$

Malek Ben Khalifa^{1,2}, Emna Sahnoun^{1,2}, Silvia Spezzano³ ,
Laurent Wiesenfeld¹ , Kamel Hammami²,
Olivier Dulieu¹ and Paola Caselli³

¹Laboratoire Aimé-Cotton, Université Paris-Saclay, CNRS, Orsay, France

²Faculty of Sciences, University Tunis El Manar Campus, 1060 Tunis, Tunisia

³CAS@MPE, Garching, Germany

Abstract. Cyclopropenylidene, $c\text{-C}_3\text{H}_2$, is a simple hydrocarbon, ubiquitous in astrophysical gases, and possessing a permanent electric dipole moment. Its readily observed multifrequency rotational transitions make it an excellent probe for the physics and history of interstellar matter. The collisional properties of $c\text{-C}_3\text{H}_2$ with He are presented here. We computed the full Potential Energy Surfaces, and we perform quantum scattering in order to provide rates of quenching and excitation for low to medium temperature regimes. We discuss issues with the validity of the usual Local Thermodynamical Equilibrium assumption, and also the intricacies of the spectroscopy of an asymmetric top. We present the wide range of actual critical densities, as recently observed.

Keywords. Collision coefficients, astrochemistry, ISM, C₃H₂, LTE

1. Introduction

Among all hydrocarbons present in the Interstellar Medium (ISM), the simplest like methane or acetylene, do not display a permanent electric dipole moment because of their high symmetry, and cannot be observed by usual rotational spectroscopy. They can be seen only thanks to their intense IR spectra, at temperatures high enough to excite the transition, or else, with high enough an IR background to see the transitions in absorption. For the low temperatures usually characteristic of the ISM ($T \lesssim 200$ K), few simple hydrocarbons are observables. The most common closed shell one is a carbene molecule, displaying a divalent carbon atom, cyclopropenylidene, $c\text{-C}_3\text{H}_2$. It has been widely observed in emission for a long time, thanks to its intense rotational spectrum, with usual lines observed from the 3 mm to the sub-mm bands, covering most telescopes from GBT to ALMA.

In order to quantify abundances of observed molecules, it is necessary to make the correspondence between the observed line intensities and the density/column densities of the molecule, not a simple task. Besides the issues pertaining to optical depth, one must also have a handle on the rotational temperature of the species, allowing to make an estimate of the population of the various rotational levels. The population of those levels is governed by the interplay of photon emission and absorption, on the one hand, and collisions with the main gases present, often H_2 (even if H, He and e^- are of importance). If the rates due to collisional excitation/quenching are high enough, the internal temperature (T_{rot}) and the kinetic temperature (T_{kin}) are equal, allowing for the so-called LTE (Local Thermodynamical Equilibrium) approximation to hold. Otherwise $T_{\text{rot}} \neq T_{\text{kin}}$,

allowing for non equilibrium processes to occur, like masing or overcooling. The dividing point is the critical density of colliders, defined here for the transition $f \leftarrow i$ as:

$$n^*(\text{H}_2/\text{He}) = \frac{A_{fi}}{k(T)_{fi}} \quad (1.1)$$

Here we wish to present the rates of collisional processes pertaining to $c\text{-C}_3\text{H}_2$, in collision with He, for moderate kinetic temperatures. The important point to discuss is the estimation of n^* , hence, the validity of the LTE approximation.

2. Methods

We have computed recently the interaction potential of $c\text{-C}_3\text{H}_2$ with both H_2 and He (Ben Kahlifa *et al.* (2019a); Ben Kahlifa *et al.* (2019b)) by means of very precise quantum chemistry *ab initio* methods, in the Born-Oppenheimer and rigid molecules approximations. We made use of the coupled cluster formalism augmented with a perturbative treatment of the short-range behaviour of the dielectronic wave-function (CCSD(T)-F12a, Werner & Knowles (1985)), using the MOLPRO quantum chemistry code. The *ab initio* points were computed for a dense grid of the intermolecular degrees of freedom, a regular grid for intermolecular distances, a Monte-Carlo importance sampling grid for the relative angular positions (2 or 4 angles). The resulting cloud of *ab initio* points was subsequently fitted onto relevant functionals, and entered into the quantum dynamics code (Molscat in its OpenMP version, Molscat (2011)). The dynamics is performed on the full dimensionality (3 or 5), by means of the time-independent Coupled-Channel method or the Coupled States approximations for higher collision energies (see Ben Kahlifa *et al.* (2019a) for all details). The resulting energy dependent inelastic cross sections $\sigma_{fi}(E_{\text{coll}})$ are averaged over a Maxwellian distribution of kinetic energy, yielding the $k_{fi}(T)$ that enters into equation 1.1.

3. Results

Rates. We present rates for collisions of ortho- $c\text{-C}_3\text{H}_2$ with He in Fig. 1. While Helium is a collision partner of its own, it is customary to use it as a proxy for H_2 , for computing collisions with He is at least one order of magnitude lighter than with H_2 , both for Potential Energy Surface computation and for dynamics (the latter, if $j(\text{H}_2) > 0$). In that case, a mass correcting factor is applied (lower kinetic velocity of He with respect to H_2).

Critical densities. In order to discuss the relevance of the LTE approximation for computing the abundances and excitation temperature of $c\text{-C}_3\text{H}_2$, we present in Fig. 1 an analysis of the critical densities of several transitions of $c\text{-C}_3\text{H}_2$, observed very recently. The color coding, which covers 8 orders of magnitude for the Einstein A coefficient, underlines the crucial importance of a good knowledge of the spectroscopy of the observed molecule (see also the recent paper on partition functions, Carvajal *et al.* (2019)).

The usual approach to analysing the rotational lines is to use the LTE approximation to all lines, or at least to groups of lines within a range of frequency. For a simple rotor (like CO or HC_3N), there is a simple correlation between the frequency, the J -value and the A coefficient: Neglecting the centrifugal distortion, the frequency of the transition increases linearly with J , and the A coefficient increases as J^3 . Assuming slower variations of the k coefficients (for the optically allowed transitions), as a first approximation, n^* scales as J^3 . Note that this completely neglects collisional transfer of population outside of optically allowed transitions, an approximation which is not allowed in most complex situations, especially so when combined with optical depth effects (see a vivid description in the manuals of the CASSIS software, which has been developed by IRAP-UPS/CNRS (<http://cassis.irap.omp.eu>)).

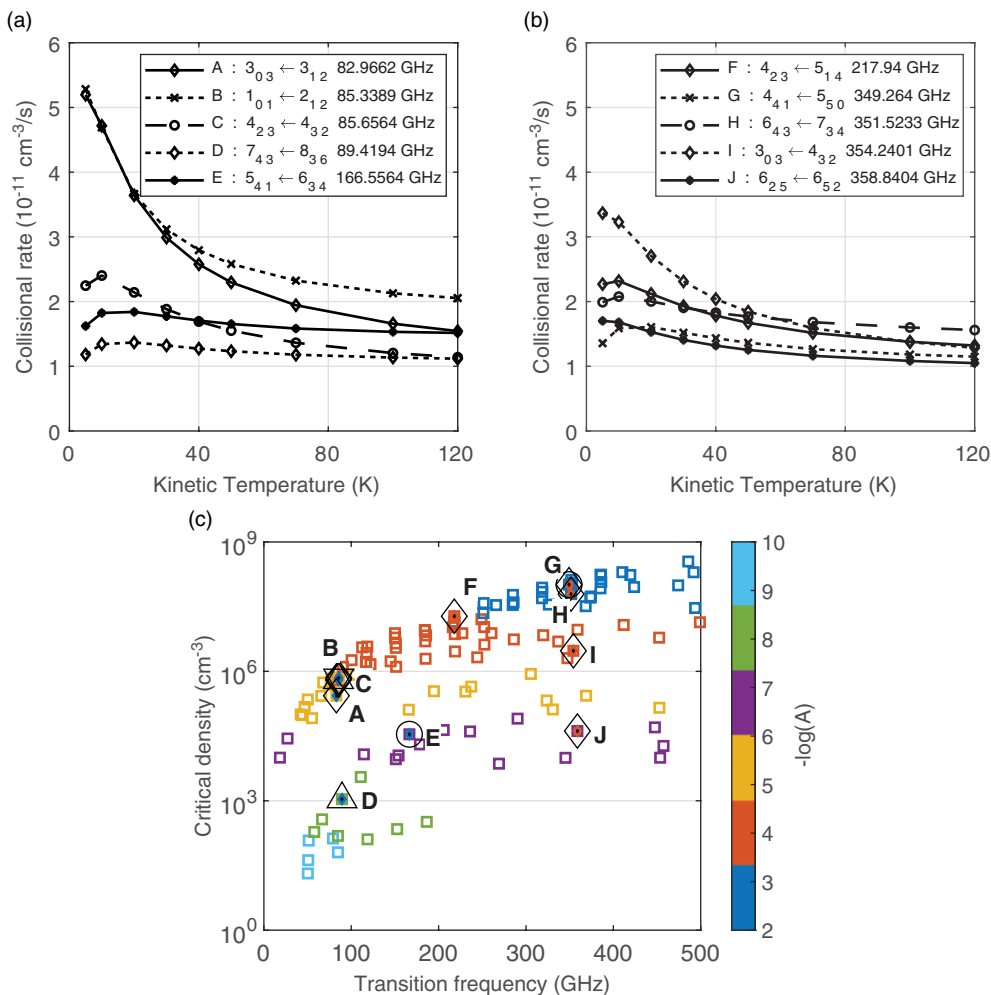


Figure 1. (a) and (b) Quenching rates for the optically allowed transition, as described in the captions, for the collision ortho- c - C_3H_2 -He, rates scaled for mass effects. (c) Critical densities for all optically allowed transitions, at frequency usually observed (40 to 500 GHz). Note the very large range of the densities. Temperature, 20K. The color labelling follows the value of the $-\log_{10}(A)$ Einstein coefficients (in sec^{-1}). Black symbols denote observed transitions, whose quenching rates are given in panels (a) and (b). Observation references: A-B-D, [Schmidt *et al.* \(2018\)](#); C, [Guzmán *et al.* \(2018\)](#); E, [Higushi *et al.* \(2018\)](#); F-H-I-J, [Murillo *et al.* \(2018\)](#); G, [Artur de la Villarmois *et al.* \(2018\)](#).

Here (like for other asymmetric rotors like H_2O for example), there is no correlation between quantum numbers, frequencies and A values. One sees it readily in Figure 1. Even more so, while transition frequency remains nearly constant, the critical density varies wildly, 3 orders of magnitude for the 3mm IRAM band, 5 for the sub-mm ALMA. Consequently, when plotting the usual rotational diagram, while some transitions may fall down on the line of simple rotational diagram, some lines may be off, because of the very different spectroscopic and collisional properties. One must be especially aware that the selection rules for the electric dipole allowed transitions are especially permissive ($\Delta J = 0, \pm 1$, $\Delta K_a, \Delta K_c = \pm 1, 3, 5, \dots$), resulting is strongly or weakly allowed transitions (compare transitions G and J for example). A precise analysis must of that relies on the intimate knowledge of spectroscopy and also on the quenching rates.

4. Conclusion

Quenching rates of $c\text{-C}_3\text{H}_2$ have been recently computed. We use them here to discuss the critical density for various observed transitions of $c\text{-C}_3\text{H}_2$. It is clear that (i) many optical depth effects and (ii) more advanced treatments of the interplay collisions-photon emission/absorption are just mentioned in this work. Indeed, the very simple definition of n^* is misleading. While it is true that Eq. 1.1 holds for a single two-level system, the actual analysis is more complex, and very often population cascades through the levels by means of collisional processes forbidden by optical transitions. Such a situation is all the more probable for the asymmetric rotors, hence no full correlation exist between level energies and quantum numbers. The use of quenching coefficients combined with optical depth effects and modelling of the source is often the only way to understand the very intricate line shapes observed in many astrophysical environments.

References

- Artur de la Villarmois, E., Kristensen, L. E., Jørgensen, J. K., Bergin, E. A., Brinch, C., Frimann, S., Harsono, D., Sakai, N., & Yamamoto, S. 2018, *A&A*, 614, A26
- Ben Khalifa, M., Sahnoun, E., Wiesenfeld, L., Khadri, F., Hammami, K., Dulieu, O., Spezzano, S., & Caselli, P. 2019, *PCCP*, 21, 1443
- Ben Khalifa, M., Wiesenfeld, L., & Hammami, K. 2019, *PCCP*, 21, 9996
- Carvajal, M., Favre, C., Kleiner, I., Ceccarelli, C., Bergin, E., & Fedele, D. 2019 *A&A*, 627, A65
- Guzmán, A. E., Guzmán, V. V., Garay, G., Bronfman, L., & Hechenleitner, F. 2018, *ApJS*, 236, 45
- Higuchi, A. E., Sakai, N., Watanabe, Y., López-Sepulcre, A., Yoshida, K., Oya, Y., Imai, M., Zhang, Y., Ceccarelli, C., & Lefloch, B. 2018, *ApJS*, 236, 52
- Molscat 2011 website : <http://faculty.gvsu.edu/mcbaneg/pmpmolscat/>
- Murillo, N. M., van Dishoeck, E. F., Tobin, J. J., Mottram, J. C., & Karska, A. 2018, *A&A*, 620, A30
- Schmidt, D. R., Zack, L. N., & Ziurys, L. M. 2018, *ApJL*, 864, L31
- Werner, H. J. & Knowles, P. J. 1985, *J. Chem. Phys.*, 82, 5053